Performance of S+C+L-Band Transmission over Single-Mode Fibers in Accordance with ITU-T Recommendation with Backward Distributed Raman Amplifiers

Kohei Saito
NTT Network Innovation Laboratories
Nippon Telegraph and Telephone Corp.
Yokosuka, Japan
kohei.saito.nw@hco.ntt.co.jp

Fukutaro Hamaoka
NTT Network Innovation Laboratories
Nippon Telegraph and Telephone Corp.
Yokosuka, Japan
fukutaro.hamaoka.xz@hco.ntt.co.jp

Masanori Nakamura
NTT Network Innovation Laboratories
Nippon Telegraph and Telephone Corp.
Yokosuka, Japan
masanori.nakamura.cu@hco.ntt.co.jp

Akira Masuda
NTT Network Innovation Laboratories
Nippon Telegraph and Telephone Corp.
Yokosuka, Japan
akira.masuda.hf@hco.ntt.co.jp

Takayuki Kobayashi
NTT Network Innovation Laboratories
Nippon Telegraph and Telephone Corp.
Yokosuka, Japan
takayuki.kobayashi.wt@hco.ntt.co.jp

Etsushi Yamazaki
NTT Network Innovation Laboratories
Nippon Telegraph and Telephone Corp.
Yokosuka, Japan
etsushi.yamazaki.wk@hco.ntt.co.jp

Yoshiaki Kisaka
NTT Network Innovation Laboratories
Nippon Telegraph and Telephone Corp.
Yokosuka, Japan
yoshiaki.kisaka.dc@hco.ntt.co.jp

***Abstract*— Transmission evaluations in an 18.6-THz triple-band configuration over 100 km showed the low water-peak G.652.D fiber obtained better transmission performance with higher Raman gain for the S-band than the low-loss large-core cut-off shifted G.654.E fiber.**

Keywords— digital coherent, optical multi-band transmission, backward distributed Raman amplifier

I. INTRODUCTION

Many of recent researches have focused on wideband wavelength division multiplexing (WDM) using the bandwidth from the S- to L-band, providing an effective solution for high-capacity transmission [1, 2]. In the ultra-wideband WDM configuration, inter-channel stimulated Raman scattering (SRS) limits wideband optical transmission leading to the signal quality deterioration of shorter-wavelength signals [3]. Low-loss large-core cut-off shifted fiber (CSF) compliant with ITU-T G.654.E should be a better choice to increase the capacity and transmission distance [4]. It has recently been reported that there is a potential application of triple-band (S, C, and L bands) WDM [2] and Raman amplification [2, 5, 6] even if the wavelength of the WDM signals and Raman pumping light exist in the cable cutoff region (<1530nm) for CSF. In the case of the triple-band WDM transmission, the wavelength of the Raman pumping light for the S-band signals has the same wavelength band as the hydroxyl absorption peak (1383 nm) in standard single mode G.652.B fiber (SSMF) and CSFs. Therefore, there is a possibility that sufficient Raman gain cannot be obtained for the S band through CSF (G.654.E) transmission.

In this paper, we experimentally evaluate the performance of S+C+L-band transmission over 100 km with or without backward-pumped distributed Raman amplification (DRA) for the S band with respect to different fiber types; We compare the transmission performance with the widely commercially available SSMF (G.652.B), low water-peak single-mode fiber (LWPF) (G.652.D), and CSF (G.654.E) (see the attributes in table 1). Our experimental comparison shows that the system setup of the LWPF with 1390-nm backward-pumped DRA achieves a better signal-to-noise ratio (SNR) of the signal for the S band than that of the CSF and SMF after 100-km transmission. We also calculated the net bitrate of the S-band signal with 136-GBd 64 quadrature amplitude modulation (QAM) using a rate-adaptive coding technique [7]. The results show that the net bitrate of 996 Gb/s for the S-band signal at 1470.472 nm through the LWPF was higher than that of 946 Gb/s through the CSF and that of 826 Gb/s through the SSMF.

Table 1. Attributes of fibers in accordance with ITU-T Recommendation

Attribute	G.652.B (SSMF)	G.652.D (LWPF)	G.654.E (CSF)
Attenuation Coefficient (1550 nm) [dB/km]	≤0.35	≤0.30	≤0.23
Attenuation Coefficient (1383 nm) [dB/km]	-	≤0.40	-
Cable cutoff wavelength [nm]	≤1260	≤1260	≤1530
Chromatic dispersion (1550 nm) [ps/(km･nm)]	Typ. 17.0	≤18.6	≤23.0
Typical mode field diameter [μm]	9.5 (1310nm)	9.2 (1310nm)	11.5 (1550nm)

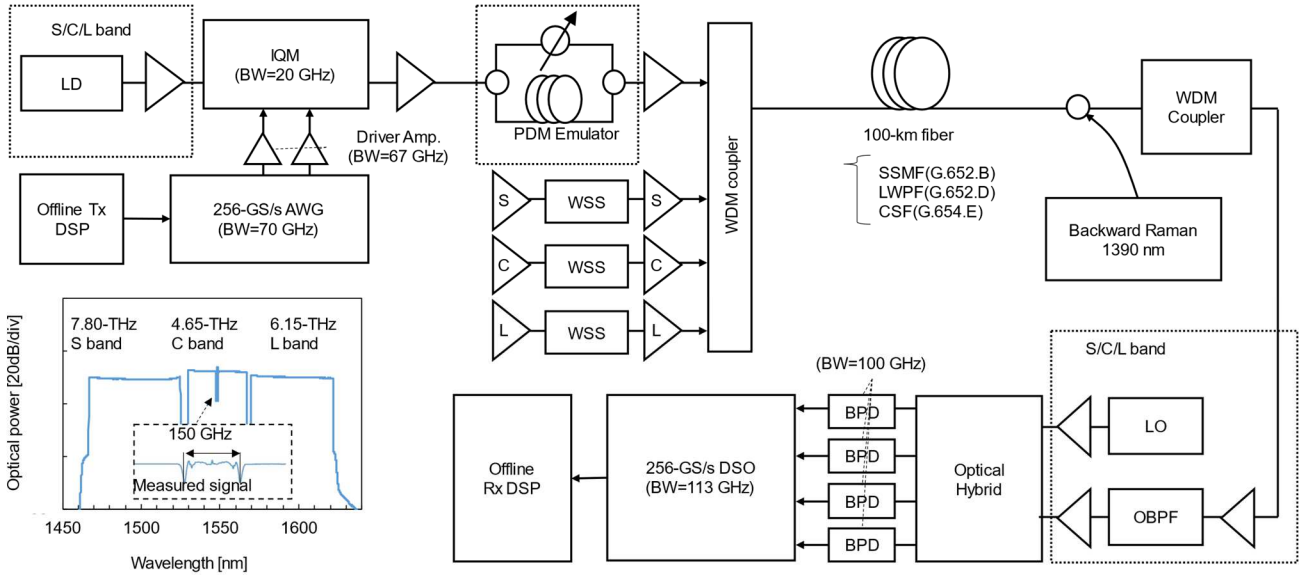

Fig.1 Experimental setup for S+C+L band signal transmission and transmitted WDM signal spectra of 18.6-THz bandwidth.

II. Experimental Setup

Figure 1 shows the setup for S+C+L-band transmission experiments. A transmitter for the measured optical signal consists of an offline transmitter-side (Tx) digital signal processing (DSP), 256-GS/s arbitrary waveform generator (AWG), driver amplifiers, and an in-phase quadrature modulator (IQM). A receiver has a coherent receiver consisting of an optical hybrid and balanced photo detectors (BPDs), 256-GS/s digital sampling oscilloscope (DSO), and an offline receiver-side (Rx) DSP. Laser diodes (LD) sources for the signal and local oscillator (LO) were external cavity lasers for the S and L bands, and integrable tunable laser assemblies (ITLAs) for the C band. The measured signals for the S, C, and L bands were generated by switching the LD sources, optical amplifiers, and optical band-pass filters in the optical transmitter and receiver. The electrical signals of 136 Gbaud generated in the Offline-DSP were output from the AWG. The signals through the driver amplifiers were then modulated in the LN-IQM with the optical carrier output from the LD. The modulation format of the measured signal was PDM-64QAM. The carrier frequency of the measured signal was set to 1470.472, 1482.470, 1494.665, 1520.824 nm in the S band, 1534.054, 1548.315, 1562.844 nm in the C band, and 1573.920, 1595.277, 1617.222 nm in the L band. We used thulium-doped fiber amplifiers (TDFAs) for the S band and erbium-doped fiber amplifiers (EDFAs) for the C and L bands. The S-, C-, and L-band WDM signals were emulated using amplified spontaneous emissions from the TDFAs and EDFAs, whose power spectra were flattened using a gain equalizer (GEQ) based on flexible-grid wavelength selective switches (WSS). Then, the WDM signals in the S, C, and L bands were multiplexed in a WDM coupler as a 150-GHz-grid triple-band WDM signal with a total bandwidth of 18.6 THz (see the inset of Fig. 1).

Transmission lines were 100-km SSMF (G.652.B), LWPF (G.652.D), and CSF (G.654.E). Attributes of the fibers are shown in Table 1. The fiber loss coefficient of 100 km that we measured is shown in Fig. 2 as the red dashed line for SSMF, the blue dashed line for LWPF, and the green dashed line for CSF. For LWPF, a small water peak due to hydroxyl absorption of less than 0.4 dB/km within the specification of ITU-T G.652.D can be observed around 1383 nm. On the other hand, SSMF (G.652.B) and CSF (G.654.E) have a loss coefficient of >0.5 dB/km around 1383 nm. Fiber input power in the S, C, and L bands were 18.6, 19.5, and 20.8 dBm, respectively; the total fiber input power of the triple-band WDM signal was 24.5 dBm. Under this condition, as shown in Fig. 3, a maximum optical power penalty of 6.2 dB for SSMF, 6.1 dB for LWPF, and 4.6 dB for CSF occurred in the presence of inter-band SRS. To compensate for the excess

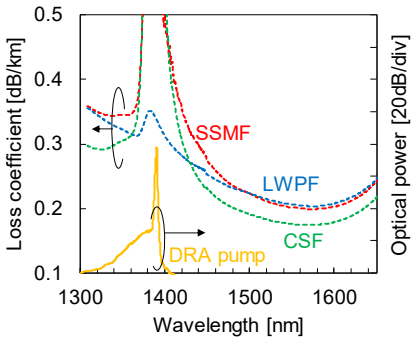

Fig.2. Attenuation coefficient of fibers and spectra of the 1390-nm backward-pumped DRA light.

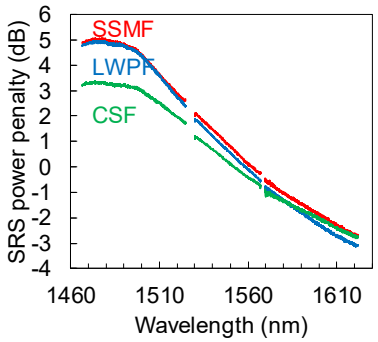

Fig.3. Power penalty by inter-channel SRS.

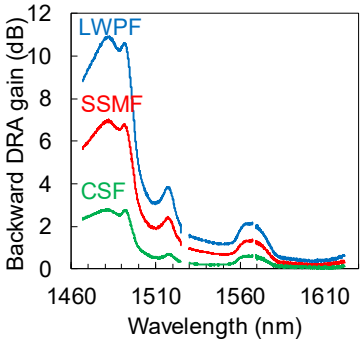

Fig.4. Spectra of the backward DRA gain with the 1390-nm pump light.

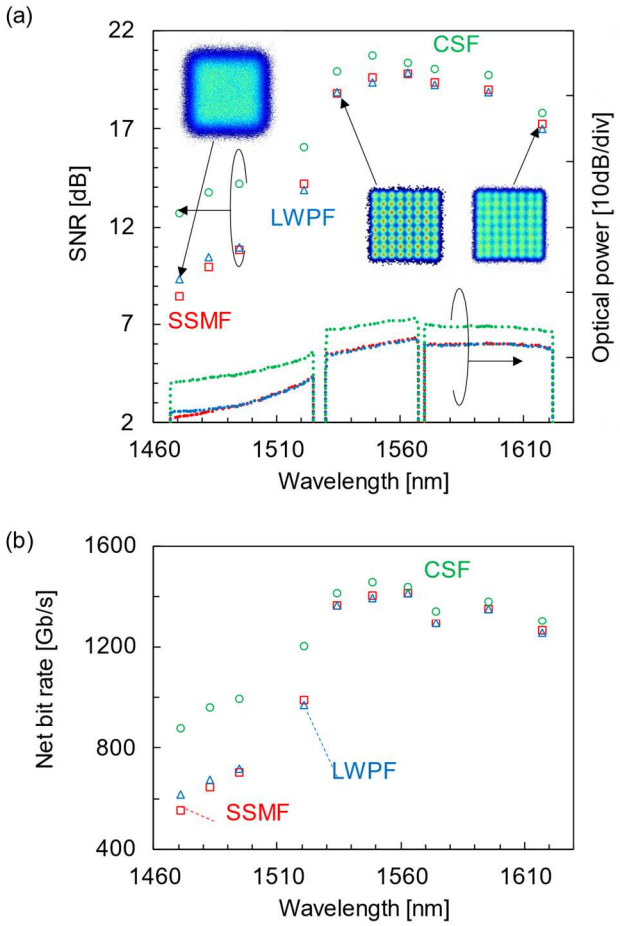

Fig.5. (a) SNR, spectra, and (b) net bitrate after S+C+L-band 100-km transmission without backward-pumped DRA. The constellations show the 136-GBd 64QAM signals at 1470.472, 1534.054, 1617.222 nm for LWPF (G.652.D) transmission.

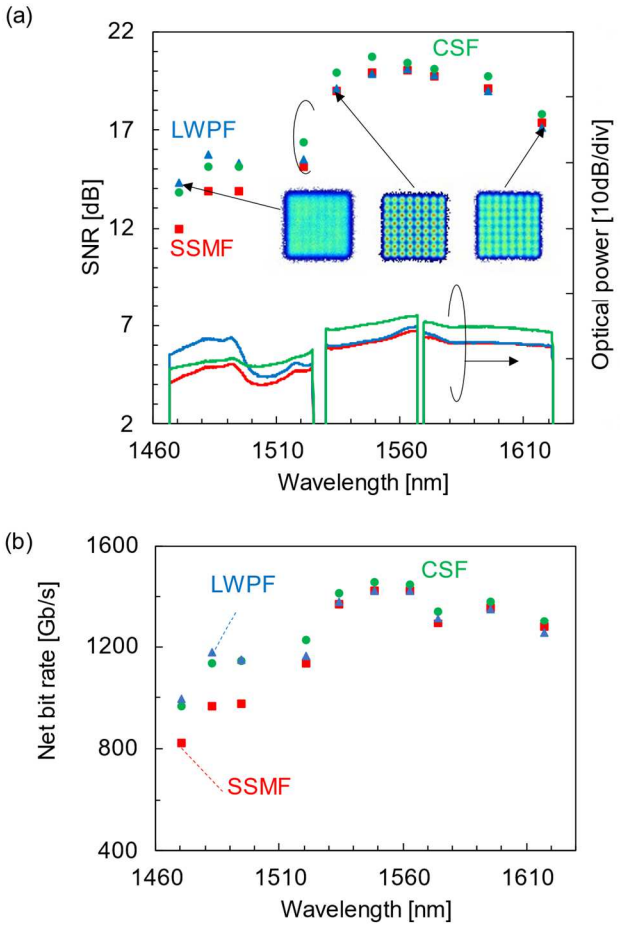

Fig.6 (a) SNR, spectra, and (b) net bitrate after S+C+L-band 100-km transmission with backward-pumped DRA. The constellations show the 136-GBd 64QAM signals at 1470.472, 1534.054, 1617.222 nm for LWPF (G.652.D) transmission.

power loss by the inter-band SRS, we applied a BW-pumped DRA at 1390 nm with 250 mW. The spectra of the backward-pumped Raman light are shown in Fig.2 as the orange dashed line. Fig. 4 shows the gain of a backward-pumped DRA amplification. The maximum DRA gain of 10.8 dB was obtained for LWPF (G.652.D). Due to a much larger water peak caused by hydroxyl absorption around 1383 nm for SSMF (G.652.B) and CSF (G.654.E) than that for LWPF, the DRA gain was reduced to 6.8 dB for SSMF and 2.6 dB for CSF.

After 100-km transmission, the triple WDM signal was divided into each S-, C-, and L-band WDM signal. Then, the WDM signals were amplified by a TDFA for the S band and EDFAs for the C and L bands at the receiver side to compensate for the transmission losses. After filtering the measured signal for each S, C, and L band using a flexible grid WSS, the signal was detected with the coherent receiver and digitized in the DSO. In the Rx-DSP, a frequency domain 8×2 MIMO adaptive equalizer simultaneously compensated for the Tx- and Rx- linear responses of the received signal [8].

III. Results and Discussion

SNR, optical spectra, and net bitrate after the triple-band (S, C, and L bands) transmission over 100-km SSMF (G.652.B), LWPF (G.652.D), and CSF (G.654.E) without and with the 1390-nm backward-pumped DRA are shown in Fig. 5(a) and 5(b), respectively. An increase of optical power due to the Raman on-off gain of 6.4 dB for SSMF, 9.0 dB for LWPF, and 3.6 dB for CSF was observed in the short wavelength side of the S band under the presence of inter-channel SRS. We measured the SNR of 10 channels in the WDM signal to evaluate the signal quality. Without backward-pumped DRA as shown in Fig. 5(a), the short-wavelength-side channel of the S band signal at 1470.472 nm through SSMF fiber shows the lowest SNR of 8.6 dB due to inter-channel SRS. The SNR at 1470.472 nm through LWPF was also low at 9.4 dB. The S-band channels have lower SNR compared to the C and L bands due to the large fiber attenuation coefficient, and small amplifier saturated output power. On the other hand, as shown in Fig. 5(b), the SNR in the S band through LWPF was drastically improved at more than 14.3 dB because the 1390-nm backward-pumped DRA worked very well due to the small water peak of less than 0.4 dB (see Fig. 2) from the specification of ITU-T G.652.D. For SSMF and CSF, however, the effect of the backward-pumped DRA was limited due to the excess loss in the water peak region around 1383 nm. We also evaluated the net bitrate of the 136-Gb/s 64QAM signals which were calculated from the required code rate based on the rate-adaptive coding technique [7]. In 18.6-THz S+C+L-band transmission with 1390-nm backward-DRA amplification, for LWPF, the net bitrate of 996 Gb/s was achieved at 1470.472 nm thanks to the sufficient Raman gain with a reduced water peak according from ITU-T G.652.D. This net bitrate is higher than the 946 Gb/s through the CSF and the 826 Gb/s through the SSMF.

IV. CONCLUTIONS

We experimentally evaluate the performance of 18.6-THz S+C+L-band transmission over 100 km with or without backward-pumped DRA in terms of different fiber types compared with the SSMF (G.652.D), LWPF (G.652.B), and CSF (G.654.E). Our experimental comparison shows that the system setup of LWPF fiber with backward-pumped DRA achieves a better SNR for the S band than that for CSF and SMF after 100-km transmission due to the sufficient Raman gain with a reduced water peak of less than 0.4 dB according to ITU-T G.652.D. From the analysis of net bitrate based on a rate-adaptive coding technique after 100-km transmission of 136-GBd 64 QAM signals, a net bitrate of 996 Gb/s at 1470.472 nm in the S band is achieved. This net bitrate is higher than the 946 Gb/s through the CSF and the 826 Gb/s through the SSMF. The experimental results indicate that the LWPF compliant with ITU-T G.652.D is a promising candidate for applying ultra-wideband transmission technologies thanks to the low cable cutoff wavelength (≤1260 nm) and low water peak (≤0.4 dB) at 1383 nm.

REFERENCES

[1] B. Feng, L. Gan, Q. Guo, S. Cao and X. Xiao, "Performance Evaluation of S+C+L-Band Optical Transmission over G.652.D and G.654.E Fibers," in Conference on Lasers and Electro-Optics, Technical Digest Series (Optica Publishing Group, 2022), paper JW3B.105, 2022.

[2] F. Hamaoka, K. Saito, A. Masuda, H. Taniguchi, T. Sasai, M. Nakamura, T. Kobayashi and Y. Kisaka, "112.8-Tb/s Real-Time Transmission over 101 km in 16.95-THz Triple-Band (S, C, and L Bands) WDM Configuration," in Proceedings 27th OptoElectronics and Communications Conference (OECC) and 2022 International Conference on Photonics in Switching and Computing (PSC), PDP-A-3, 2022.

[3] M. A. Iqbal, L. Krzczanowicz, I. Phillips, P. Harper and W. Forysiak, "150nm SCL-Band Transmission through 70km SMF using Ultra-Wideband Dual-Stage Discrete Raman Amplifier," 2020 Optical Fiber Communications Conference and Exhibition (OFC), W3E.4, 2020.

[4] F. Buchali, V. Aref, M. Chagnon, R. Dischler, H. Hettrich, R. Schmid and M. Moeller, "52.1 Tb/s C-band DCI transmission over DCI distances at 1.49 Tb/s/λ," 2020 European Conference on Optical Communications (ECOC), doi: 10.1109/ECOC48923.2020.9333182, 2020.

[5] M. Mlejnek, J. D. Downie and M. O'Sullivan, "Examination of Potential Terrestrial System Effects From Raman Pumps Below Cable Cutoff in G.654.E Fibers," in Journal of Lightwave Technology, vol. 37, no. 17, pp. 4282-4294, 1 Sept.1, 2019.

[6] Y. Yamamoto, "Practical Aspects of G.654.E Fibers for Terrestrial Long Haul Transmission," in Optical Fiber Communication Conference (OFC) , OSA Technical Digest (Optica Publishing Group, 2019), paper Tu3J.1, 2019.

[7] M.Nakamura, M. Nagatani, T. Jyo, F. Hamaoka, M. Mutoh, Y. Shratori, H. Wakita, T. Kobayashi, H. Takahashi, Y. Miyamoto, "Over 2-Tb/s Net Bitrate Single-carrier Transmission Based on >130-GHz-Bandwidth InP-DHBT Baseband Amplifier Module" in Proceedings The European Conference on Optical Communication (ECOC), Th3C.1, 2022.

[8] M. Nakamura, K. Kobayashi, F. Hamaoka, and Y. Miyamoto, "High Information Rate of 128-GBaud 1.8-Tb/s and 64-GBaud 1.03-Tb/s Signal Generation and Detection Using Frequency-Domain 8×2 MIMO Equalization," in Optical Fiber Communication Conference (OFC) , OSA Technical Digest (Optica Publishing Group, 2022), paper M3H.1, 2022.